

# DISCRETE NUMERICAL MODELLING OF SINGLE-PARTICLE CRUSHING AND OEDOMETRIC TESTS FOR DIFFERENT VALUES OF SUCTION

JOÃO MANSO\*, JOÃO MARCELINO\* AND LAURA CALDEIRA\*

\*Geotechnical Department (DG)  
National Laboratory for Civil Engineering (LNEC)  
1700-066, Lisbon, Portugal  
e-mail: [jmanso@lnec.pt](mailto:jmanso@lnec.pt), web page: <http://www.lnec.pt/>

**Key words:** Discrete Element Method, Crushing tests, Oedometer tests, Rockfill, Suction stresses

**Abstract.** Particle breakage plays an important role in rockfill mechanical behaviour. Under compression or shear, the crushing of particles modifies the grain size distribution and indirectly, the material permeability, their frictional properties and the corresponding critical state. In order to study the breakage of individual particles, several approaches were adopted using discrete element method (DEM). Some considered sub-particles joined by bonding or cohesive forces, other replaced particles, which verified a predefined failure criterion, by an equivalent group of smaller particles. In this paper, using the discrete element method, a new methodology was developed. It consisted of modelling crushable rockfill particles using the clump logic, which was responsible for providing a statistical and spatial variability in the strength and shape of the particles. Particle movements and interactions were determined using DEM, allowing to determined the deformation of the rockfill material. Clumps have a major advantage of severely decreasing the number of contact equations to be solved in the model, resulting in less computer time. A comprehensive study of the brittle failure of single-particle crushing tests is presented. Preliminary tests on particle size evolution were also performed, assuming some simplifications. No attempt was made to simulate the real particle size distribution (PSD), due to the cost of simulating smaller particles. Single-particle crushing tests and oedometer tests were simulated using crushable particles, whose results were in agreement with experimental data.

## 1 INTRODUCTION

Rockfill material is widely used in many geotechnical engineering applications, such as dams, roads, airports, and railway embankments. In particular, rockfill dams have

been increasingly used due to their inherent flexibility, capacity to cope with large seismic actions and adaptability to various foundation conditions. They have also become an economical option due to the increasing use of modern construction equipment and locally available materials. The actions originated during the construction and operation of these geotechnical structures may result in particle breakage when their crushing strength is exceeded. Several researchers have studied the influence that this phenomenon could have on the behaviour of granular materials in various geotechnical structures [1, 2, 3] and showed that, for a crushable rockfill material, particle breakage considerably influences its mechanical behaviour [4]. Under compression or shear, the crushing of particles modifies the grain size distribution, increasing the percentage of fine material [5]. Consequently, these differences in grain size distribution, and in the available range of packing densities, modify the material's permeability, its peak friction angle, and the localisation of the critical-state line in a void ratio – mean effective stress diagram [27].

In rockfill, particle sizes range from a few millimetres to over a metre, commonly leading, in rockfill dams, to mean grain size,  $D_{50}$ , in the range 0.10 – 0.40 m. Due to the large size particles of such granular materials, testing them under oedometer, simple shear or triaxial conditions would require equipment of impressive dimensions. The largest testing cells described in the literature [4, 6] were only capable of testing rockfill particles with a maximum particle size not exceeding 0.20 m [12]. A solution for this problem consists of reducing the size of the rockfill materials for testing using reduction techniques [7, 8, 9, 10, 11]. However, rockfill behaviour depends on its grain size scale, as shown by tests performed on materials with parallel grain size distributions curves but different mean grain size [12, 4]. Particle breakage controls rockfill mechanical behaviour and is affected by scale effects. The discrete element method – DEM [13] – can be an effective tool for investigating size effects, provided it is capable of properly simulating grain failure mechanisms for different stress paths [14].

Several approaches have been adopted to study particle breakage using DEM: sub-particles joined by bonding or cohesive forces [14] or replace a particle which verified a predefined failure criterion with an equivalent group of smaller particles [15]. These techniques were employed with either disks in 2D or spheres in 3D. When considering particles with general shapes, the technique consisted of bonding unbreakable and rigid sub-particles, creating a breakable particle. Then, if the bonds between these sub-particles broke, breakage occurred [16].

A natural evolution of the DEM is to be capable of reproducing the complex mechanical behaviour of granular materials, such as stiffness and crushability, and to simulate accurately the particle breakage phenomenon, despite the complexity of the particle shapes considered.

The main purpose of this paper is to present a new methodology capable of simulating crushing tests and oedometer compression of a rockfill, with the advantages of low computation costs and truthfully simulating the material behaviour. Firstly, the methodology adopting crushable rockfill particles was calibrated using crushing tests performed

on rockfill materials that were collected from a dam site located in the north of Portugal. Then, the model parameters were calibrated using an oedometer test performed on specimens with a given grain size distribution. The numerical results were analysed on both the macro- and micro-scales allowing to study the role of particle breakage and the influence of stress on the compressibility of rockfill materials.

## 2 SINGLE PARTICLE CRUSHING TEST SIMULATION

### 2.1 ROCKFILL MECHANICAL BEHAVIOUR

During some particle-crushing tests performed by Nakata et al. [17], they observed differences between the force-displacement relationships of particles with different materials and crystalline structures, leading them to define two types of failure. The first one, which was related to the crushing of asperities, was defined by the first point at which the load slipped, which they represented by  $F_c$ . The second one was the peak force that originated the major splitting of the particle, causing its failure, represented by  $F_f$ .

In order to better understand the mechanisms that take place in a particle during a crushing test, it is necessary to study the particle behaviour relatively to its stress state and fracture conditions (initiation and progression). By placing a rockfill particle between two rigid platens, it is possible to directly measure its crushing strength by simple compression. McDowell and Bolton [18] and Nakata et al. [17] used this technique to analyse the behaviour of single sand particles, and adopted the definition of the particle strength proposed by Jaeger et al. [19]. Adopting the nomenclature used by Nakata et al. [17], the crushing strength,  $\sigma_f$ , can be determined by dividing the maximum force,  $F_f$ , measured during the crushing test that led to particle breakage, by the square of the initial distance between platens,  $h_0$ :

$$\sigma_f = \frac{F_f}{h_0^2} \quad (1)$$

Weibull [20] proposed the following mathematical expression for the survival function,  $S_\Sigma$ , of particles of volume  $V$  given a stress  $\sigma$ :

$$S_\Sigma(\sigma) = 1 - F_\Sigma(\sigma) = P(\Sigma > \sigma) = \exp \left[ - \left( \frac{\sigma}{\sigma_0} \right)^m \right], \sigma \geq 0 \quad (2)$$

where  $\sigma_0$  is the characteristic value associated with a probability of survival of 37 % (considering that  $\sigma = \sigma_0$  in Eq. 2 becomes  $S_\Sigma(\sigma_0) = 1/e$ ) and  $m$  is the Weibull modulus.  $1/m$  is a measure of dispersion of  $\Sigma$ .

When the applied stress is null ( $\sigma = 0$ ) all particles survive ( $S_\Sigma = 1$ ) and, as the stress increases, particles begin to fail, reducing the value of  $S_\Sigma$ . Eventually, it is possible to crush all particles simply by increasing the stress, therefore  $S_\Sigma \rightarrow 0$  when  $\sigma \rightarrow \infty$ .

The Weibull modulus characterises the effect of size on failure, such that the characteristic value,  $\sigma_0$ , is a function of the volume  $V$  according to Lim et al. [28]:

$$\sigma_0 \propto V^{-1/m} \quad (3)$$

A material with a Weibull modulus  $m$  equal to 100 may be considered as having a well-defined asperity crushing or particle breakage strength. There are some Weibull moduli adopted for various materials. For traditional ceramic materials such as bricks and tiles,  $m$  can have values smaller than 3 (large dispersion), whereas for materials having less dispersion in strength, such as metals and other alloys,  $m$  can have values near 100 [21].

It is possible to determine the characteristic values for particle breakage ( $\sigma_{f0}$ ) and Weibull moduli ( $m_f$ ) experimentally, simply by testing samples of different size ranges and plotting the results. The characteristic value ( $\sigma_{f0}$ ) can be determined graphically for each curve, but the Weibull modulus ( $m_f$ ) must be obtained by curve fitting. Applying logarithms twice in both sides of Eq. 2, it can be rewritten as:

$$\ln \left[ \ln \left( \frac{1}{S_{\Sigma}(\sigma)} \right) \right] = m \ln \left( \frac{\sigma}{\sigma_0} \right) \quad (4)$$

and the Weibull modulus can be determined by simply calculating the slope of the corresponding linear regression line.

Another interesting feature of the Weibull theory is that it allows the study of the volume dependency of  $S_{\Sigma}$ . As previously shown,  $S_{\Sigma_{V_0}}$  is the survival probability of a particle of volume given a stress  $\sigma$ . Consequently, the probability that  $n$  particles survive that stress is  $[S_{\Sigma_{V_0}}]^n$ , considering  $\sigma$  an independent variable. If those  $n$  particles are enclosed in a single particle of volume  $V = nV_0$ , its survival probability should remain  $[S_{\Sigma_{V_0}}]^n$ , i.e.:

$$S_{\Sigma_V}(\sigma) = [S_{\Sigma_{V_0}}]^n = [S_{\Sigma_{V_0}}]^{V/V_0} \quad (5)$$

Considering that the strength of a brittle solid depends upon the smallest value of strength of a number of cracks,  $r$ , within the solid, Yoshinaka et al. [29] showed that the solid strength is given by the mode,  $\tilde{\sigma}$ , determined based on the smallest extreme value density function of  $r$  cracks. This mode is given by:

$$\tilde{\sigma} = \frac{1}{(r\sigma_0^{-m})^{1/m}} \left( \frac{m-1}{m} \right)^{1/m} \quad (6)$$

Assuming that the number of cracks in the solid is proportional to its volume, i.e.  $r_0/r = V_0/V$ , the relation between the strength and volume of the solid becomes:

$$\tilde{\sigma} = \frac{1}{(r\sigma_0^{-m})^{1/m}} \left( \frac{m-1}{m} \right)^{1/m} \quad (7)$$

where  $V$  represents the volume of the particle,  $V_0$  is a volume of a standard-size particle and  $m$  represents the Weibull modulus.



Lee [30] has shown that the average crushing stress is a function of particle size,  $d$ . Based on experimental data, an expression can be obtained expressing the effect of size on  $\sigma_f$ :

$$\sigma_f \propto d^\alpha \quad (8)$$

where  $\alpha$  is an empirical parameter, typically negative. Then, according to the statistical theory proposed by Weibull [20], the survival probability,  $S_\Sigma(\sigma)$ , of a particle of size,  $d$ , subjected to a crushing stress,  $\sigma$ , is given by:

$$S_\Sigma(\sigma) = \exp \left[ - \left( \frac{d}{d_0} \right)^{n_d} \left( \frac{\sigma}{\sigma_0} \right)^m \right] \quad (9)$$

where  $d_0$  represents a reference size. This equation is based on the weakest link concept, which states that the probability of non-failure of a chain of length  $d$  under uniaxial stress is equal to the probability of non-failure of every link of length  $d_0$ . Therefore, the term of Eq. 9 refers to the scale ratio and indicates the number of links of the chain.  $n_d$  represents the geometric similarity of the mechanical problem, and is equal to 1, 2 or 3, for one-, two- or three-dimensional similarities.

Considering a survival probability and known empirical parameters, the size effect relation between the induced crushing stress at failure,  $\sigma_f$ , and the size of the specimen,  $d$ , is given by McDowell and Bolton [18] and Ovalle et al. [22]:

$$\sigma_f \propto d^{n_d/m} \quad (10)$$

The verification of this relation results in the empirical validation of Weibull's theory. In particular, a value of  $n_d = 3$  has usually been adopted for compression tests of rockfill particles performed between two rigid parallel platens [18], assuming an isotropic homogeneous material and that failure occurred under bulk induced crushing stress. However, these assumptions do not always occur.

Considering  $k = 3/m$ , the corresponding average crushing strength will be as follows:

$$\sigma = \sigma_0 \left( \frac{d}{d_0} \right)^{-k} \quad (11)$$

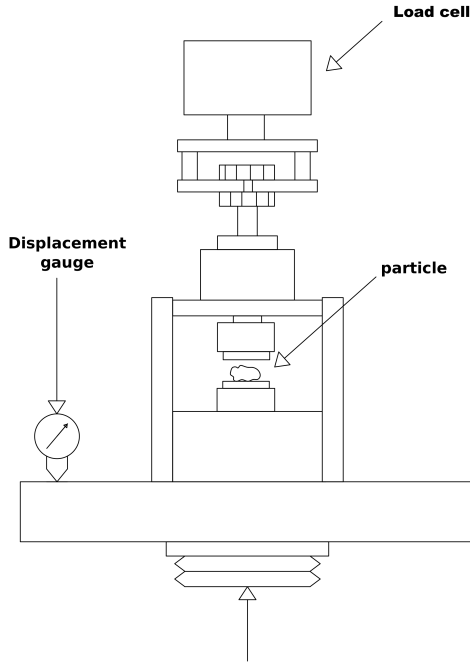
This relation allows us to predict the effect of the particle size on the crushing strength.

## 2.2 Material properties

The material tested was a granite used in the construction of Veiguihas dam, a rockfill dam located in the Montesinho Natural Park, with a bulk density of 2400 – 2540 kg/m<sup>3</sup> and an apparent porosity of 2.4. The sizes of rockfill particles used for testing ranged from 9.5 to 50.4 mm, divided into four intervals: 9.5–19.1, 19.1–25.4, 25.4–38.1, and 38.1–50.4 mm. The material presented a weathering state W2-3, with natural water content between 0.24 and 0.28 %, and a maximum water content around 1.0 %.

### 2.3 Single-particle crushing tests

Figure 1 shows the apparatus used to perform the single-particle crushing tests. This equipment was developed in Laboratório Nacional de Engenharia Civil (LNEC) and its main components consisted of: the axial loading ring, the steel platens and the axial displacement measuring devices (which included a digital and analogue displacement transducer, for redundancy). The test consisted of placing a rockfill particle between two rigid steel platens (with a guide rail to ensure verticality), and then applying an axial force on the particle until it broke, by moving the lower platen at a constant rate (0.306 mm/min). The platens were 75 mm in diameter and two load rings were used: one for smaller particles (9.5 – 19.1 and 19.1 – 25.4 mm), with 4.9 kN capacity and a resolution of 0.5 N, and another for particles with larger sizes (25.4 – 38.1 and 38.1 – 50.4 mm), with a capacity of 49.0 kN and a resolution of 5.0 N. Thirty crushing tests were carried out for each rockfill particle size interval, totalling 120 tests. During each crushing test, force and displacement were measured. Details of the single-particle crushing tests performed for other conditions can be found in Manso et al. [32].



(a) Apparatus scheme



(b) Apparatus

Figure 1: Particle crushing apparatus

Figure 2 presents four force-displacement curves and Figure 3 shows the rockfill particles, after the respective crushing test, for each size range. These are typical examples of

the behaviour observed for small (9.5 – 19.1 and 19.1 – 25.4 mm) and large particles (25.4 – 38.1 and 38.1 – 50.4 mm). Some similarities can be found between these curves, such as small decreases in load ( $F_c$ ) that occurred before the particle breakage ( $F_f$ ), which may be related to the crushing of asperities. On the other hand, the curves of the small particles were almost linear, even after the occurrence of small load decreases, whereas in the case of large particles the curves were generally non-linear.

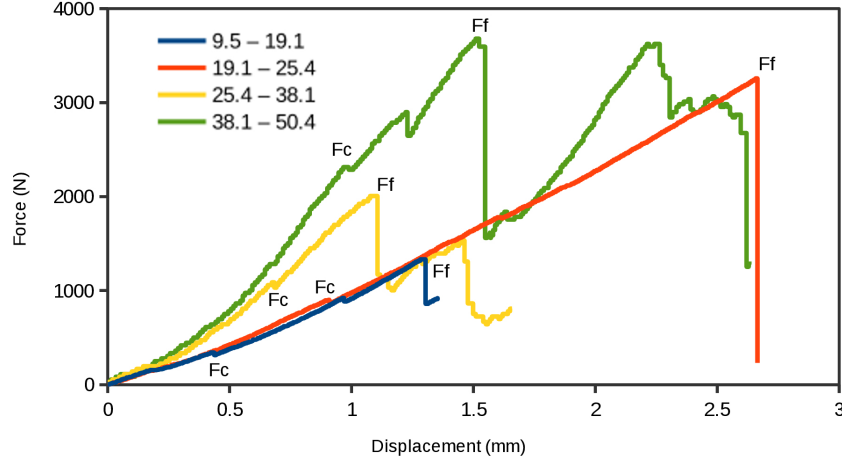


Figure 2: Force-displacement curves

## 2.4 Statistical analysis

Figure 4 presents the experimental cumulative frequency curves of survival, with a sample size of 30 ( $S_{30}(\sigma_f)$ ), obtained for each particle size interval. Small particles (9.5 to 19.1 mm) had the largest crushing strength, though there was no clear tendency regarding the other dimensions. It can be observed that the maximum stresses that originated total particle breakage ranged from 8 to 16 MPa.

The curves shown in Figure 5 are obtained by dividing the results presented in Figure 4 by their respective characteristic value,  $\sigma_{f0}$ . This representation almost overlapped the curves, which exhibited similar behaviour, meaning that the particle size did not have much influence on the material dispersion, for the studied sizes.

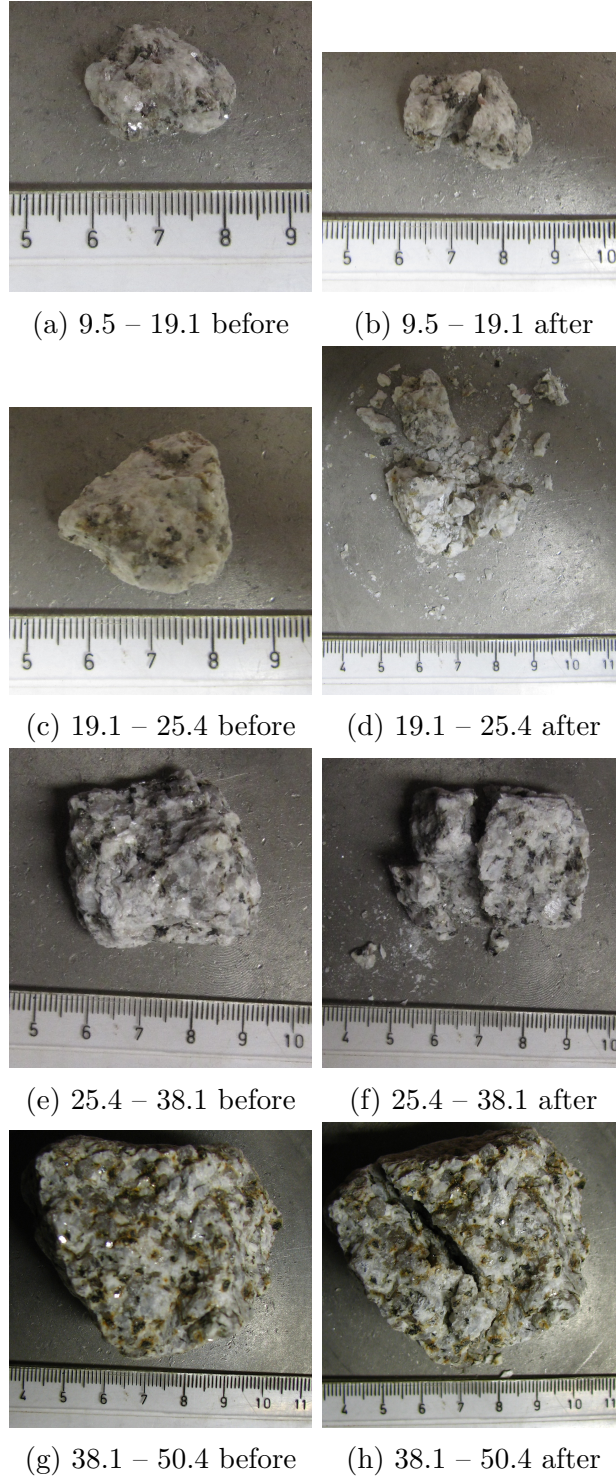


Figure 3: Rockfill particles before and after crushing tests for each size range

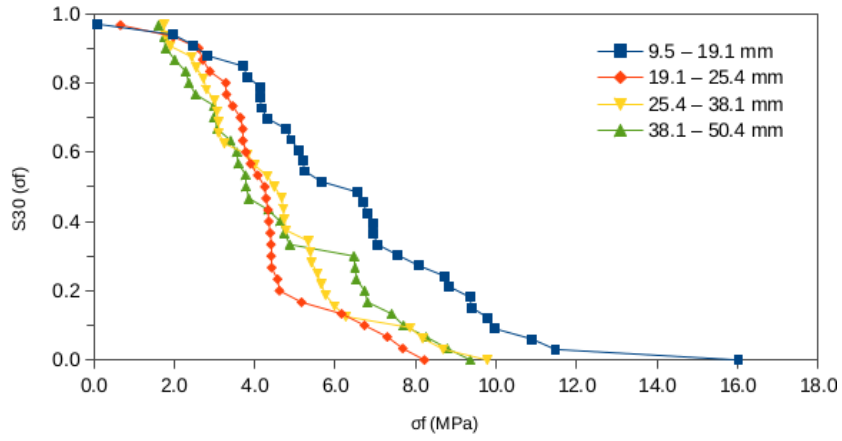


Figure 4: Survival probability curves for several dimensions

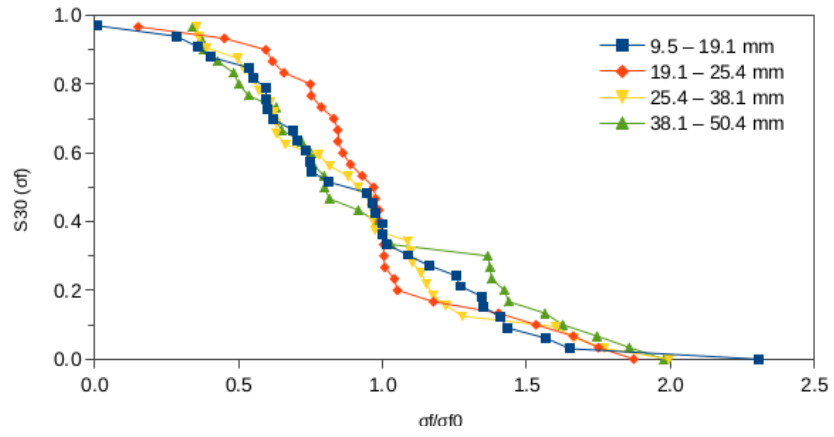


Figure 5: Normalized survival probability curves for several dimensions

The values obtained for the characteristic value and Weibull modulus ranged from 4.39 to 6.95 and 2.20 to 3.21, respectively, for the particle breakage ( $\sigma_{f0}$  and  $m_f$ ). The results are shown in Table 1. Considering the results of all the performed single-particle crushing tests, a coefficient  $m_f$  of 2.43 was obtained for particle breakage.

Table 1: Characteristic value and Weibull modulus for the particle breakage

Dimensions [mm]	$\sigma_{f0}$	$m_f$
9.5 to 19.1	6.95	2.29
19.1 to 25.4	4.39	3.21
25.4 to 38.1	4.90	2.58
38.1 to 50.4	4.73	2.20
9.5 to 50.4	5.33	2.43

To test the fitting to the experimental results, a Kolmogorov-Smirnov test was performed to evaluate the appropriateness of the proposed Weibull distribution model considering the experimental data. Although the significance level has no physical meaning, it should be selected with care, since the characteristic value and Weibull modulus are random variables estimated from a finite sample. Values as low as 5 % are often selected for the significance level in many engineering applications. The values obtained for the maximum discrepancy between the empirical and theoretical cumulative frequencies,  $D_{30}$ , are presented in Table 2. For a sample size of 30, the critical values,  $D_{30}^\alpha$ , for various significance levels,  $\alpha$ , can be easily found in the bibliography. Apart from rockfill particles with dimensions between 19.1 and 25.4 mm, which returned a maximum discrepancy of 0.21 for the particle breakage ( $D_{30}^{0.10} = 0.22$ ), the maximum discrepancies obtained are less than the critical value at a 20 % significance level ( $D_{30}^{0.20} = 0.19$ ), meaning that the respective theoretical Weibull distributions are acceptable at that significance level.

After performing this statistical analysis, the results obtained were used to calibrate the developed numerical models and assess their capabilities.

Table 2: The Kolmogorov-Smirnov Test for the particle breakage

Dimensions [mm]	$D_{30}, \sigma_f$
9.5 to 19.1	0.12
19.1 to 25.4	0.21
25.4 to 38.1	0.10
38.1 to 50.4	0.14

### 3 OEDOMETER COMPRESSION SIMULATION

#### 3.1 Oedometer compression tests

The oedometer tests were also performed in LNEC facilities on a well-graded rockfill, using a cell with a height of 0.474 m and a diameter of 0.5 m (Figure 6). The loading and unloading phases were divided into ten steps (100 kPa) of 8 hours up to 1 MPa, by moving the lower platen at a constant rate (0.14 mm/s). Two different conditions were analysed, a specimen was flooded (RH = 100 %) and the other was in equilibrium with a relative humidity of 50 %. Details of the specimens preparation can be found in Manso [31]. During each test, force and displacement were measured.



Figure 6: Oedometer apparatus

#### 3.2 Rockfill mechanical behaviour

Cundall and Strack [13] found that only a number of heavily loaded chains of particles respond to an externally applied stress, which had been observed experimentally by Oda and Konishi [23], whereas the remaining particles within the mass are only slightly loaded. Their main contribution to the system is the stabilisation of the main loading chains. This



can be observed in Figure 7, where the light grey contact forces represent the results of two different loading steps (0.5 and 1.0 MPa vertical stress) with the beginning of the test (0.1 MPa vertical stress). While some contact forces increased with the vertical stress (main loading chains), others kept the same value during the test (stabilisation forces). In a rockfill specimen, particles are supported by nearby particles, increasing its coordination number (average number of contacts per particle). This aspect should distribute stresses along its contacts, leading to a reduction in crushing stress, when compared to single-particle crushing tests [18]. Therefore, particles in a rockfill specimen might break at an applied stress even higher than the crushing strength.

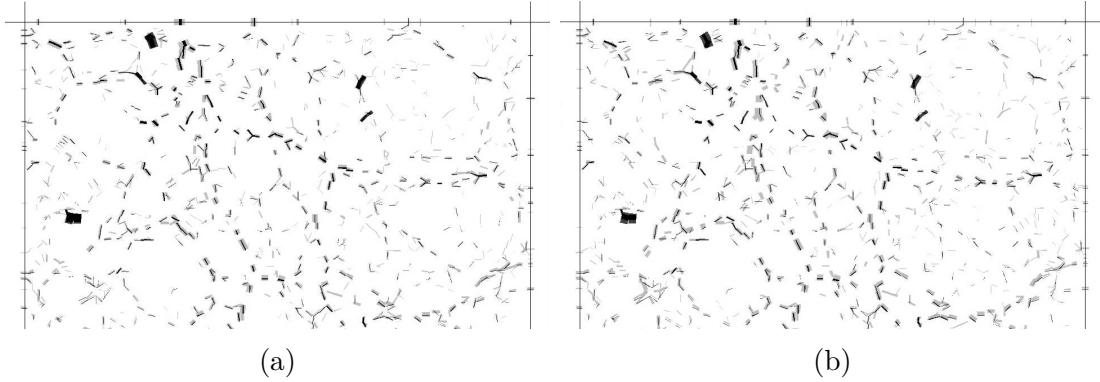


Figure 7: Schematic comparison of the contact forces during oedometer tests (detail), black forces refers to the results of a vertical stress of 0.1 MPa and the light grey contact forces refer to an axial stress of: a) 0.5 MPa, b) 1.0 MPa.

### 3.3 Specimen generation

Rockfill particles were created and loaded in order to verify the applicability of the presented simulation approach. The objective of the present model was to simulate the material response during an oedometer test and to reproduce its grain size evolution. The rockfill particles could break if their strength was exceeded and their shape would change due to the broken fragments that remained in the simulation.

The numerical simulation started by creating an initial set of exo-disks placed randomly with a size slightly smaller than required, without overlaps (Figure 8a). After that, they were expanded to the final size and cycled until equilibrium was reached, reducing unwanted gaps. Table 3 presents the characteristics of the numerical specimen. Following Cheng et al. [14] and Robertson [24], the shear stiffness and the friction coefficient were reduced to zero, while the lateral wall stiffness was reduced ten times ( $5 \cdot 10^7$  N/m) and the initial normal stiffness was increased 100-fold ( $5 \cdot 10^{10}$  N/m), during the process of preparing the specimen.

Following the same methodology adopted in the modelling of single-particle crushing tests, each exo-disk was replaced by a regular assembly of disks in hexagonal close pack-



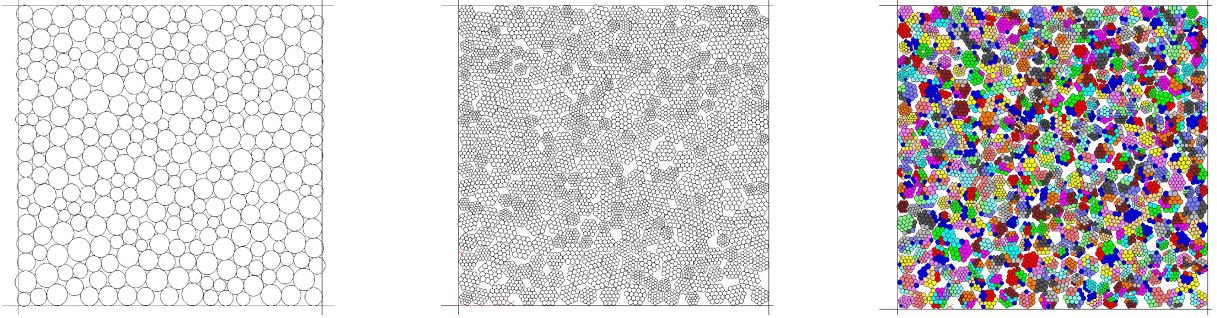


Figure 8: Methodology applied to generate rockfill particles and respective rockfill specimen. a) exo-disks, b) elementary disks and c) clumps

Table 3: Characteristics adopted to simulate the oedometer specimen

Input parameter	Numerical value
Height [m]	0.474
Width [m]	0.500
$D_{min}$ [mm]	19.1
$D_{max}$ [mm]	38.1
Clump size [mm]	$10.0 \pm 0.2$
Density [ $\text{kg/m}^3$ ]	2052
Normal stiffness [N/m]	$5 \cdot 10^8$
Wall stiffness [N/m]	$5 \cdot 10^8$

ing, where the radius of the disks within this assembly was 20 % of the original exo-disk (Figure 8b). Then, the clump logic was continuously activated until all particles were clumped (Figure 8c). The new specimen was cycled again until equilibrium was reached. In order to reduce the possibility of breaking the bonds during the preparation of the specimen, their strengths were initially set very high ( $10^9$  Pa) and the shear and normal stiffness were set to  $9 \cdot 10^6$  N/m. This objective was achieved and no bonds broke during the specimen preparation process, after introducing the clumps, for an equilibrium stress of 5 kPa. Before starting the test, bond strengths were fixed to their final value ( $10^3$  MPa), the contact shear and normal stiffness were set to  $2 \cdot 10^{10}$  N/m and the friction coefficient was set to 0.5, corresponding to a contact friction angle of  $26.5^\circ$ . The differences of behaviour, regarding different relative humidity conditions, were matched by setting different values for normal and shear bond stiffness of parallel bonds (Table 4).

Figure 8c shows the layout of particles used in this simulation. In the oedometer test the specimen was vertically loaded while restraining lateral deformation by using rigid walls. The model comprised 317 numerical rockfill particles, 1520 clumps and a total of

Table 4: Properties adopted for the numerical simulation

Input parameter	Numerical value	
Relative humidity [%]	50	100
Normal and shear bond stiffness (parallel bonds) [N/m]	$0.95 \cdot 10^8$	$1.1 \cdot 10^8$
Normal and shear bond strength (parallel bonds) [MPa] [mm]	$1 \cdot 10^3$	
Radius multiplier (parallel bonds)	0.5	
Normal and shear bond stiffness [N/m]	$2 \cdot 10^{10}$	
Friction coefficient	0.5	

6023 elementary disks. These numbers were chosen to originate a model that achieved reasonable computation times and was capable of properly simulating the material behaviour. The oedometer test consisted of ten loading stages of 100 kPa until it reached 1 MPa. During each loading stage, the top and bottom walls moved progressively together, fixing the position of the other pair of walls to achieve the desired boundary conditions. The displacement rate of the walls was limited to a maximum value in order to reach the desired stress. The stress was determined by summing and averaging all contact forces on the top wall. The voids ratio was calculated considering the solids volume as the total area of the circles, resulting in an initial value of 0.26, which is of the same order of magnitude as the real rockfill (0.29).

It is clear that modelling particle breakage using a 2D representation has some limitations (in both single-particle crushing and oedometer tests), being the particle rearrangement in the oedometer test the most relevant. The fundamental assumption in PFC2D is simulating particles as disks having finite thickness and placing them in a single layer toward out of plane direction, similar to the plane strain condition. However, since the out-of-plane forces and displacements are not considered into the force-displacement law, the conditions in the simulation are neither plane strain nor plane stress [25]. Therefore, no attempts were made to match the voids ratio in PFC2D material with the 3D physical material. Nonetheless, it will be assumed that a 2D analysis is reasonably accurate.

Several velocity-limited loading tests were performed in order to check for possible inertia effects on the location of the virgin compression line. Then, it was decided to adopt a velocity of 0.01 m/s, since it was considered slow enough to eliminate rate effects, due to any bouncing that could occur initially for unloaded rockfill particles.

### 3.4 Oedometer compression simulation

The specimen was loaded by continuously increasing the vertical stress up to 1 MPa. In Figure 9 the registered axial stress and the percentage of broken bonds were plotted and it could be observed that irrecoverable compression was registered beyond 100 kPa. Moreover, for the range of stresses simulated, the behaviour could be mainly attributed

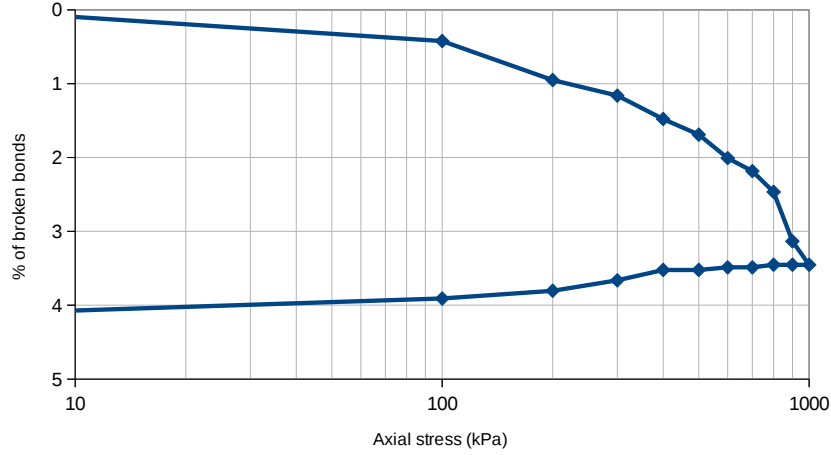


Figure 9: Percentage of bonds broken against axial stress, during oedometer compression simulation

to particle rearrangement, since only 3.5 % of bonds broke. During unloading (swelling curve) of the simulated rockfill specimen, the behaviour was inelastic and the bond breakage practically ceased. The observed marginal breakage might result from particle rearrangement, where the asperities could cause bond stresses greater than the maximum crushing stress allowed, despite the decrease of the macroscopic stress. Figures 10 and 11 present the evolution of the PSD's for both the experimental test (initial and final curves, represented respectively by the red and blue lines) and the numerical simulation (indicated in the figure, for each loading stage). This allowed to analyse the evolution of the PSD, at each loading stage, which was impossible in the experimental test, and it could be observed that no stage stood out, for both relative humidity conditions. The evolution was gradual. No attempt was made to simulate the real PSD, since the modelling of the smaller particles (less than 1 mm) would severely increase the computational cost, if not even impossible to simulate without having numerical instabilities.

Figures 10 and 11 also compares oedometric compression curves between the experimental test and the DEM simulation with a platen speed of 0.01 m/s, for each relative humidity condition. Although compressibility was clearly different, for both conditions, simulations were capable of capturing the essential of material behaviour. During loading, both shapes are similar and the DEM simulations capture the transition from particle rearrangement, due to elastic compression, into what may be described as clastic compression. Clastic yielding happens when the applied stress causes the onset of particle crushing, assuming that the onset of particle breakage leads to the bending of the normal compression line, causing the rapid increase of the material compressibility index [26]. During unloading, the simulated rockfill also showed good similarities with the laboratory test.

These results show that the presented simulation approach was generally capable of

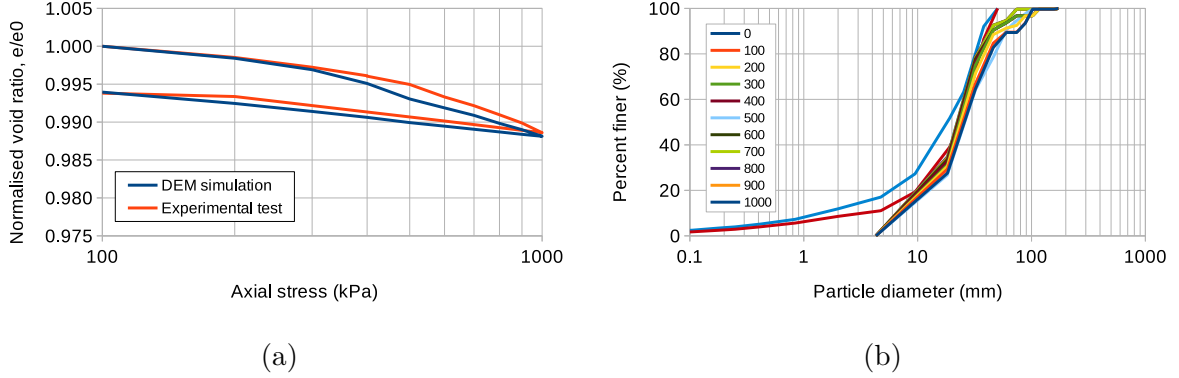


Figure 10: Results obtained by numerical modelling: a) percentage of bonds broken against axial stress, for different limiting platen speeds; b) the evolution of the PSD's (experimental test and numerical simulation)

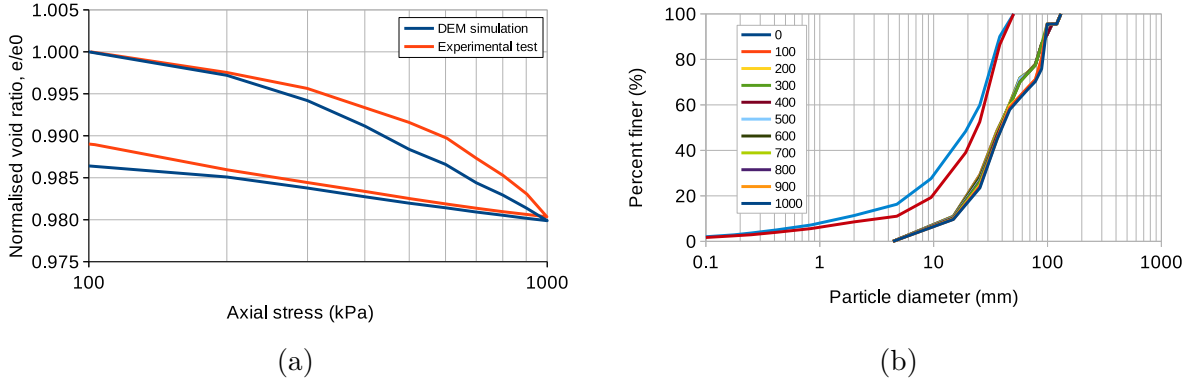


Figure 11: Results obtained by numerical modelling: a) percentage of bonds broken against axial stress, for different limiting platen speeds; b) the evolution of the PSD's (experimental test and numerical simulation)

describing the oedometer compression response.

## 4 CONCLUSIONS

This work presents a fundamental investigation of rockfill behaviour, due to an increased interest regarding both the effect of the relative humidity in the mechanical behaviour of rockfill and its modelling using particle discrete element method.

In the particle-crushing tests, two different behaviours were observed for small and large particles. The curves of the small particles were almost linear, even after the occurrence of small load decreases, whereas in the case of large particles the curves were generally non-linear. Single-particle crushing test results were interpreted using the Weibull statistics, which was found capable of fitting the relationship between the crushing strength and

the survival probability. Nonetheless, in this work, Kolmogorov-Smirnov tests, at the 5 % significance level, were performed to evaluate the appropriateness of the proposed Weibull distribution model considering the experimental data. Results verified the acceptability of this distribution to study the experimental data.

The single-particle crushing tests and the oedometer compressibility on the rockfill was generally approached through DEM modelling, following careful specimen preparation and defining the parameters based on laboratory test results. The developed model adopted clump logic to simulate rockfill particles, allowing them to randomly subdivide into smaller shapes. This was achieved by introducing the idea that a rockfill particle can be considered to be a group of bonded micro-elements, here represented as clumps. Breakage occurred in the rockfill particles when a bond between clumps broke. This methodology allowed to obtain better results, providing more realistic load-deformation response. However, it also obtained realistic strengths and was capable of studying the particle size evolution in the oedometer test.

The validity of the developed methodology was verified by modelling the crushing strength of a real particle following the Weibull distributions. The numerical simulations mimicked the experimental tests in several aspects and also showed their importance in study the mechanics of the single-particle crushing test, including the failure process. This feature was also observed during the modelling of the oedometer test. The presentation of the contact forces between particles, for different loading steps, showed the evolution of some heavily loaded chains, in response of an externally applied stress, supported by small chains.

There are some limitations of the model, since a 2D representation was used. The most relevant one was regarding the particle rearrangement in oedometer test. Despite those limitations, the methodology was able to capture the shape of the oedometer compression curve, obtained in laboratory, as well as, the transition from particle rearrangement into elastic compression. These similarities were also present during unloading.

## REFERENCES

- [1] Lee K. and Farhoomand I. (1967) Compressibility and crushing of granular soil in anisotropic triaxial compression. *Canadian Geotechnical Journal* IV(1).
- [2] Zeghal M. (2009) The impact of grain crushing on road performance. *Geotechnical and Geological Engineering* 27(4): 549–58.
- [3] Okada Y., Sassa K and Fukuoka H (2004) Excess pore pressure and grain crushing of sands by means of undrained and naturally drained ring-shear tests. *Engineering Geology* 75(3-4): 325–43.
- [4] Marsal R.J. (1967) Large-scale testing of rockfill materials. *Journal of the Soil Mechanics and Foundation Division, ASCE* 93(2): 27–43.

- [5] F. Casini, G.M.B. Viggiani, S.M. Springman, Breakage of an artificial crushable material under loading, *Granular Matter* 15 (5) (2013) 661–673.
- [6] Nobari E.S. and Duncan J.M. (1972) Effect of reservoir filling on stresses and movements in earth and rockfill dams. California Univ., Berkeley, Coll. of Engineering no. TE-72-1.
- [7] Zeller J. and Wullimann R. (1957) The Shear strength of the shell materials for the goschenenalp dam, Switzerland. In 4th Inst. J. on SMFE, London, UK, 399–404.
- [8] Lowe J. (1964) Shear strength of coarse embankment dam materials. 8th Int. Congress on Large Dams, 745–61.
- [9] Fumagalli E. (1969) Tests on cohesionless materials for rockfill dams. *Journal of Soil Mechanics & Foundations Division* 95(1): 313–32.
- [10] Frost R. (1973) Some testing experiences and characteristics of boulder-gravel fills in earth dams. ASTM STP 523:207, Philadelphia. 207–33.
- [11] Ramamurthy T. and Gupta K. (1986) Response paper to how ought one to determine soil parameters to be used in the design of earth and rockfill dams. Indian Geotechnical Conf., New Delhi, 15–19.
- [12] Alonso E.E., Tapias M., Gili J. Scale effects in rockfill behaviour. *Géotech Lett* 2012;2(July-September):155–60.
- [13] Cundall P. and Strack O. (1979) A discrete numerical model for granular assemblies. *Geotechnique* 29(1): 47–65.
- [14] Cheng Y., Nakata Y. and Bolton M.D. (2003) Discrete element simulation of crushable soil. *Géotechnique* 53(7): 633–41.
- [15] Tsoungui O., Vallet D. and Charmet J. (1999) Numerical model of crushing of grains inside two-dimensional granular materials. *Powder Technology* 105(1-3): 190–98.
- [16] Hosseininia E.S. and Mirghasemi A.A. (2006) Numerical simulation of breakage of two-dimensional polygon-shaped particles using discrete element method. *Powder Technology* 166(2): 100–112.
- [17] Nakata F.L., Hyde M. and Hyodo H. (1999) A Probabilistic approach to sand particle crushing in the triaxial test. *Géotechnique* 49(5): 567–83.
- [18] McDowell G. and Bolton M.D. (1998) On the micromechanics of crushable aggregates. *Geotechnique* 48(5): 667–79.

- [19] Jaeger J.C., Cook N.G.W. and Zimmerman R.W. (2007) Fundamentals of rock mechanics. John Wiley & Sons.
- [20] Weibull W. (1951) A statistical distribution function of wide applicability. *Journal of Applied Mechanics* 18: 293–97.
- [21] M. Ashby, D. Jones, *Engineering materials 2, an introduction to microstructures, processing and design*, Pergamon Press, Oxford, 1986.
- [22] Ovalle C., Frossard E., Dano C., Hu W., Maiolino S. and Hicher P. (2014) The effect of size on the strength of coarse rock aggregates and large rockfill samples through experimental data. *Acta Mechanica* 225(8): 2199–2216.
- [23] Oda M. and Konishi, J. (1974) Microscopic deformation mechanism of granular material in simple shear. *Soils and Foundations* 14(4): 25–38.
- [24] Robertson D. (2000) Computer simulations of crushable aggregates. PhD Thesis, Cambridge University.
- [25] Potyondy, D. O. and Cundall, P. A. (2004). A bonded-particle model for rock. *International journal of rock mechanics and mining sciences* 41 (8): 1329-1364.
- [26] Oldecop L. and Alonso E. (2003) Suction effects on rockfill compressibility. *Geotechnique* 53(2): 289–92.
- [27] Wood D.M. and Maeda K. (2008) Changing grading of soil: effect on critical states. *Acta Geotechnica* 3(1): 3–14.
- [28] Lim W.L., McDowell G.R. and Andrew C.C. (2004) The application of weibull statistics to the strength of railway ballast. *Granular Matter* 6(4): 229–37.
- [29] Yoshinaka R., Osada M., Park H., Sasaki T. and Sasaki K. (2008) Practical determination of mechanical design parameters of intact rock considering scale effect. *Engineering Geology* 96(3-4): 173–86.
- [30] Lee D, (1992) The angles of friction of granular fills. PhD dissertation, Cambridge University.
- [31] Manso, J. (2017) Predicting the behaviour of rockfill embankments. PhD Thesis. Instituto Superior Técnico, Lisbon.
- [32] Manso, J., Marcelino, J. and Caldeira, L. (2021) Single-particle crushing strength under different relative humidity conditions. *Acta Geotechnica* 16.3 (2021): 749-761.